POLYMER IMAGING WITH FRESNEL PROJECTION MICROSCOPY

VU THIEN BINH[1], V. SEMET[1] and N. GARCIA[2]

[1)] Laboratoire d'Emission Electronique, DPM-URA CNRS
Université Claude Bernard Lyon 1, 69622 Villeurbanne, France
[2)] Fisica de Sistemas Pequenos, CSIC
Universidad Autonoma de Madrid, CIII, 28049 Madrid Spain

ABSTRACT. The use of nanotips as atom-sources of electrons in a projection microscope is described. The specific characteristics of the e-beam which are attached to the atomic size of the source are fully exploited in a compact low-energy electron microscope: the Fresnel Projection Microscope. Images of nanometric fibres of carbon and of polymers, which show details less than one nanometer with observation voltages around 200 V, are presented and discussed.

1. Introduction

Observations of macromolecules, synthetic and biological, using mostly Atomic Force Microscopy (AFM) were thoroughly discussed at this workshop in numerous presentations. The advantage of AFM over classical electron microscopy rests mainly on the absence of interaction between a high-energy electron beam with the specimen. The main obstacle in obtaining high-resolution electron microscopy images of organic specimens is the radiation damage, caused primarily by inelastic electron scattering. This induces breakage of the chemical bonds and subsequent destruction of the specimens.

We present, here, an alternative approach to the observation of organic specimens based on the use of a nanotip as an atom-source of electrons [1,2] in a projection microscope [3]. This combination takes advantage of the simplicity and low working voltage of the projection microscope (50-30OV) and the unique properties of the electron beam field-emitted from the nanotips, that are related to the atomic size of the sources. The result is a high-resolution, low-energy electron microscope, the "Fresnel projection microscope", suited for imaging polymers with observations of details under 1 nm.

2. The projection microscope

The projection microscopy has been proposed in 1939 by Morton and Ramberg [3] with their Point Projector Electron Microscope. In 1968, E.W. Muller introduced the field ion shadow projection microscope [4] based on the same principle, which is the following. The greatly magnified shadow of an object can be obtained by making use of the quasi-radial propagation of field emitted electrons or ions coming from a tip when the object is inside the beam path. The potential of this microscopy was already perceived by the first authors [3]:"...this type of microscope involves no electron-optical lens elements, the images obtained are free from the ordinary aberrations. The limit of resolution depends solely on the distribution of initial velocities of the field electrons and on Fresnel diffraction by the object...".

The projection or shadow microscope is essentially a transmission microscope based on the radial propagation of the e-beam (Fig. 1). The image has a magnification factor M given by:

$$M = i / o \approx D / \alpha\, d \qquad (1)$$

where i and o are the image and object dimensions, D and d are the distances of the point source to the screen and the object, and the factor α is 1 or 2 without and with the diffraction respectively. Eq. (1) shows that the magnification increases by approaching the object to the tip and it can reach values in the range of 10^7-10^6 for tip-object distances between 10 nm to 100 nm, with the screen located 10 cm away from the tip. Lack of good mechanical stability has limited the magnification of the projection microscope to ~3000x for the first realisation [3], then up to ~20000x with a resolution of about 50 nm in later attempts [5,6]. With the recent technological developments of scanning tunneling microscopy (STM) [7], tip-sample distances of less than 1 nm can now be routinely handled by using piezodrives for nanometric displacements. Using this technology, it has been recently possible to observe diffraction patterns by carbon fibres, having diameters between 10 and 20 nm, in projection microscopes with magnifications of the order of 10^5-10^6 [8,9]. However, according to the authors of refs. 8 and 9, it has been only possible to have such diffraction patterns with a very efficient shielding for the ac magnetic stray field. The main argument in favour of shielding is the shiftings of the interference lines in time by the Aharonov-Bohm effect (A-B) and Lorentz force which lead to a blurring of the diffraction patterns. This argument was also used for the formation of interference patterns in the classical transmission electron microscopy (TEM) [10].

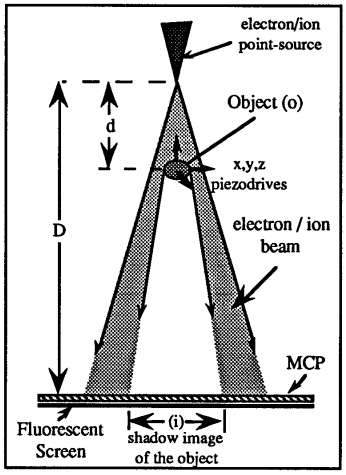

Figure 1. Schematic representation of a projection microscope.

3. The Fresnel Projection Microscope

In our projection microscope, the tip is a W-< 111> single-atom nanotip spot-welded to a Joule heating loop and in contact with a liquid nitrogen reservoir. The object holder is attached to a nanodisplacement system which is composed of a commercial piezo-motor for the z direction and home-made inertial movements for x-y displacements driven by a piezo-tube. The overall displacements are in the range of centimetres in the x, y, z directions. The resolution in the displacements is given by the minimum bending and elongation of the piezo-tube, which are in the range of 0.1 nm. The projection image is formed ~10 cm away from the tip on a multiple-channel-plate (MCP) coupled to a fluorescent screen. No magnetic shielding exists. The entire microscope system is vibration-isolated with a simple pneumatic system without any internal anti-vibration system as in STM microscopy.

The absolute dimensions of the samples and the x-y scales given in our figures are measured directly by following the displacement of the projection image on the screen versus the motion of the object due to the deflections of the sample-holder piezotube with applied voltages. The x-y dimensions of the object are then determined directly for any nanotip-object distances with an accuracy given by

the calibrations of the piezodrives whose behaviours are now very well known [7]. This procedure removed the uncertainty in the determination of the object dimensions when using Eq. (1), because the position of the virtual projection point source V (Fig. 2) is not known with accuracy due to the deformation of the electric line-field near the tip apex.

3.1. THE NANOTIPS

In the history of electron optics and electron microscopy, major instrumental development occurred with progress in the quality of the electron sources. A good example is the improvement made in the early '60s when the field-emission guns (FEG) replaced the thermionic devices in most of the electron microscopy devices. Further progress in FEG's can be made if new improvements of the field emission (FE) tip can be realised, in particular to decrease the size of the field emitting area, to increase the stability of the emission and to narrow the energy spread of the FE electrons.

Some of these behaviours were observed with nanotips as they present specific properties that are attached to the confinement of the field emission to the atomic size area at the apex [11]. Of interest for electron microscopy, they are mainly:

1) the c-beam opening is self-collimated to 4° - 6°;
2) the field emission current is very stable: variations of less than 1% have been measured for 10 hours of continuous emission;
3) the electrons come exclusively from localised bands. This leads to an energy distribution of ~100 meV at room temperature;
4) the electron beam is highly coherent [12].

Besides these advantages, a nanotip-sample distance in the range of few tens of nm leads to a FE voltage in the range of 50 to 300 V for a total current in the range of 10^{-15} - 10^{-11} A, due simply to the decrease of the FE voltage with the distance [13]. As such distances can now be obtained routinely with PZT displacements, the projection microscope is a low voltage microscope for magnifications in the range of 10^5- 10^6 without any complicated preparation technique.

3.2. THE NANOTIPS AND THE PROJECTION MICROSCOPE

We take advantage of the unique FE properties of the nanotips to push further the limits of the projection electron microscopy. Among the nanotip characteristics two are of particular interest for the improvement of projection microscopes: the protrusion geometry of the nanotips and the atomic size of the emitting area.

3.2.1. The virtual projection point

The distribution of the electric field very near the apex of a FE tip induces trajectory distortions of the emitted electrons, and thus the center of the real source at the apex does not correspond to the projection point or virtual source [10]. The virtual projection point is defined as the intersection of the asymptotes of the trajectories from the distortion free zone (far away from the tip). This is schematically drawn in Fig. 2. It is assumed as a first approximation, even if the distortions depend on the exact geometry of the tip end, that the tip behaves like a lens with a value of the ratio θ_V / θ_C around 0.5 [10]; this means that the minimum distance d_{min} from the virtual source to the apex is greater than 2 R_{apex}. As illustrated in Fig. 2, one can see from the schematic drawings that nanotips, due to its protruding geometry ending in one atom, give smaller d_{min} (around a few tens of nm) and therefore higher magnifications (of the order of 10^6) compared to hemispherical microtips.

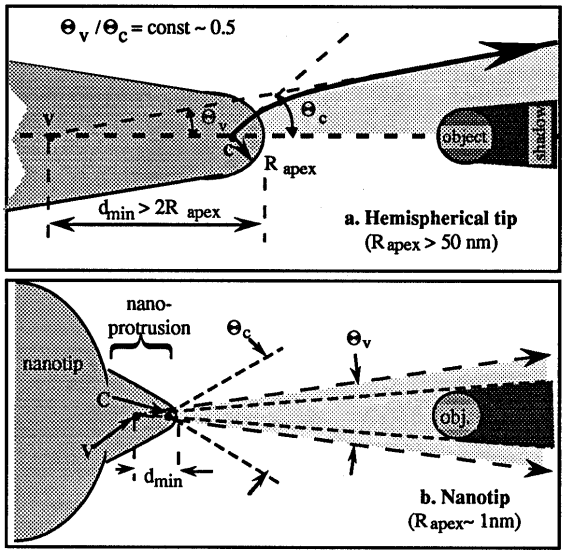

Figure 2. Field emission source models with the real emitting surface centres C and virtual projection points V

3.2.2. Fresnel or Fraunhofer diffractions

Until now we have considered the projection microscope only within the "geometrical" point of view. However, as FE beam from nanotips is coming from the last atom we have to consider also the interaction between a coherent beam [12] with an object. In other words, the diffraction of the beam by the object.

Within the projection microscope geometry, the object-screen distance is typically about 10 cm; It is therefore the distance between the tip and the object and the size of the source which will determine the nature of the resulting diffraction. As an initial approach to the problem, let us consider the classical wave theory which provides the simplest effective formalism. Imagine that we have an ideal opaque object, O, which is being illuminated by a point source, V, very close to O. Under these conditions an image of the object is projected onto the screen which is clearly recognisable despite fringes around its periphery. This is known as Fresnel or near-field diffraction, the wave-front can be considered as spherical within the object dimension. If the point source is slowly moved out or the size of the source increases, a continuous change in the fringes results. For great source-object distances the projected pattern will shrink considerably, the fringes bearing little or no resemblance to the actual object. Thereafter moving the tip-object distance changes mostly the size of the diffraction pattern and not its shape. This is Fraunhofer or far-field diffraction, the incoming wave being planar over the extent of the diffracting object. As a practical rule of thumb, Fraunhofer diffraction will prevail over Fresnel when

$$d > a^2 / \lambda \qquad (2)$$

where a is the object dimension and λ the wave-length associated to the beam. To give an order of magnitude, for λ = 0.1 run the shift between Fresnel and Fraunhofer occurs for a source-object distance of 40 nm for an object a = 2 nm, or 1 μm for a = 10 nm. In actual projection microscope, it is clear that the diffraction is neither fully Fresnel or Fraunhofer. However, the quality of the tips (fig.2) has then to be taken into account for interpreting the resulting experimental diffraction pattern. At first look and owing to its protruding geometry ending in one atom, nanotips will favour the Fresnel diffraction from nanometric objects, which is the one that gives the possibility of observing the shape of the object in the direct space.

4. Experimental results

4. 1. NANOMETRIC CARBON FIBRES

The observed samples were commercial carbon-holey films deposited on 3 mm TEM gold grids. The sample structure allows not only the observations of holes but also of carbon fibres in the range from μm down to a few nm.

As an illustrative example of the effects of the nanotip geometry on the image formation, we present in Fig.3 the diffraction pattern obtained with a carbon wire and a corresponding computer simulation. Our experimental results in Fig.3 show interference patterns that are very well explained by Fresnel diffraction by a 1.4 nm wire. The similarity between experimental and calculated Fresnel diffraction patterns indicates that the nanotips used were nearly ideal coherent point projectors.

Some former results [8] show diffraction patterns which cannot be interpreted as Fresnel diffraction. These were the case of figures A and B in La Recherche and figure 2 in J. Vac. Sci. Technol. B of ref. (8) for example. These results correspond more to a Fraunhofer diffraction of 10 to 20 nm carbon wires These diffractograms are in agreement with the underlying FEM patterns presented to obtain these fringes which were composed of multiple spots over the whole screen, that means an actual source which was not a point-source. It is in contradiction with the authors' claim [8] of a single atom point source.

The experimental results presented here have been done without any magnetic field shielding. The sharp diffraction figures obtained are experimental proofs that the projection microscope using a nanotip as coherent nanosource does not need magnetic protection in order to perform Fresnel diffraction. The measured permanent magnetic field is about 0.5 Gauss ($\sim 0.5.10^{-4}$ Tesla) with ac stray field B(ω) in the range of 1 to 5 milliGauss ($\sim 10^{-7}$ - 5.10^{-7} Tesla) nearby the microscope chamber. Under our experimental conditions, simple calculations [14] of the deviations of the image at the screen by Aharonov-Bohm and Lorentz force effects due to the stray fields give:

$$\Delta (i) \approx 2.10^{2} \times B \qquad (3)$$

with Δ(i) in meter and B in Tesla. For the measured range of the stray field B(ω), the deviations are from 20 to 100 μm. They are substantially smaller than the fringe widths at the screen which were in the millimetre range. Thus the blurring will not prevent the observation of the interference fringes. These values do not contradict our experimental results but, on the contrary, give full support to them.

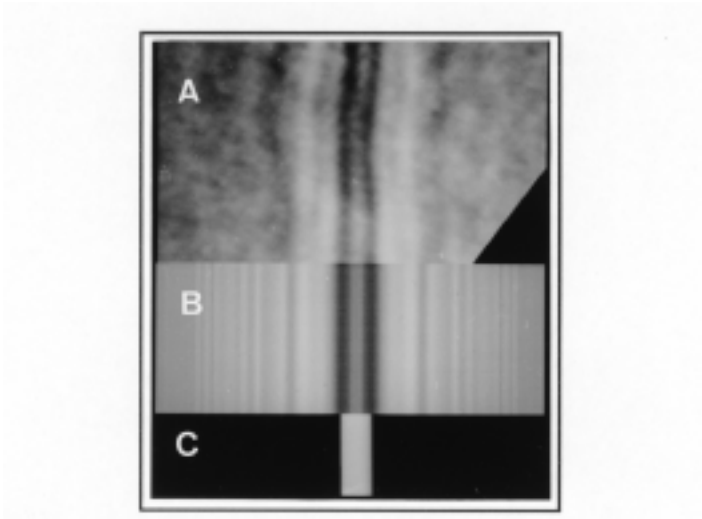

Figure 3. Fresnel diffractograms (a) Projection microscopy image of a carbon fibre at ~300 V (note the bending of the wire). (b) Calculated fringes for a straight wire with a diameter = 1.4 nm, λ = 0.7 Å, and the point source is at 28 nm from the wire. (c) The 1.4 nm wire.

4.2. POLYMERS

The FPM is then a low-voltage high-resolution microscope giving nanometric resolution in the hundred-volt energy range. It is an ideal tool for the observation of soft materials such as synthetic and bio-macromolecules.

In order to assess this prediction we have observed polymers with the FPM. The polymers were a mix of polysulfone of bis-phenol-A (PS) (95%) and polyvinylpyrrolidone (PVP) (5%) [15]. They are the constituents for the fabrication of the hollow fibres used in commercial filters for human dialysis. The specimen preparation for FPM observation is a two-step process: (1) dissolution of the polymers in chloroform to a concentration of 5.25 mg/l, then (2) deposition of 2 µl of this solution on a holey carbon gold grid. After evaporation of the solvent, the probability of having polymers stretching across a hole is rather large, allowing observation by FPM. Note that no other specimen preparation, such as staining or metal coating for example, is done.

Some conclusions on the polymer behaviour can be highlighted:

(1) For the first time, observations of polymers with details less than a nanometer can be achieved with an e-beam energies in the range of 200-300 V without any observable degradation of the sample under the beam even after one hour-duration observation.

(2) The polymer chains are self-organised into polyhedral superstructures with fibres of different lengths and different diameters, with a special mention to the presence of the nanofibres sitting across the polymer holes. The polymers form then a "gruyere cheese" like structure. The network dimensions should be related to the filtering efficiency of this material as the ultrafiltration can take place through a blocking process according to the size of the nanometric holes, and also due to the intermolecular interactions of the small particles with the surface of the polymer fibres.

(3) When the polymers are not stretched over two anchoring points, they form a clew. For the polymer this feature should be its minimum energy conformation and is observed only for polymers as opposed to carbon fibres.

(4) The Fresnel diffraction patterns of some polymer fibres show a periodic variation along the length of the structure (Fig. 4). This periodic variation has also an echo in the surrounding fringes whose patterns are more complicated than the nearly linear fringes obtained with the carbon wire (Fig. 3 for example). This is in agreement with our computer simulation results of Fresnel diffraction by a 2D periodic structure which mimics the observed shape. This raises the question of the formation of periodic supramolecular structures from the initial polymer solution as Fig. 4 suggests strongly the presence of a twist shape for the supramolecular fibre structure.

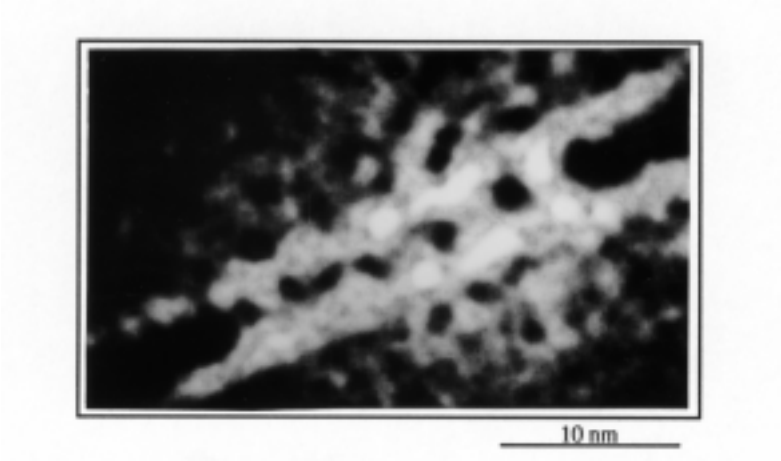

Figure 4. Fresnel diffractograms of a polymer fibre showing a periodic supramolecular structure and suggesting the presence of a twist shape.

Acknowledgements

The contributions of Dr. R. Semet and Dr. Pham Quang Tho, Service Central d'Analyse / Département Instrumentation (CNRS-Solaize), for the interpretation of the polymer images are highly appreciated. It is a pleasure to thank F. Féchet for his contribution. This work has been supported by European Community Contracts, by French and Spanish Government Agencies.

References

(1) Vu Thien Binh and N. Garcia, J. de Phys. **I1**, 605 (1991); Ultramicroscopy, **42-44**,80 (1992).

(2) Vu Thien Binh, S.T. Purcell, N. Garcia and J. Doglioni; Phys. Rev. Letters, **19**, 2504(1993)

(3) G.A. Morton and E.G. Ramberg, Phys. Rev. **56**, 705 (1939).

(4) E.W. Muller, 15th Field Emission Symposium Bonn 1968; E.W. Muller and Tien T. Tsong, in *Field Ion Microscopy: Principle and Applications*. Elsevier Publ. Co., New York, 1969, p. 129.

(5) A.J. Melmed, Appl. Phys. Letters, **12**, 100 (1968).

(6) A. Piquet, H. Roux, Vu Thien Binh, R. Uzan and M. Drechsler. Rev. Phys. Appl. **5**, 645 (1970).

(7) For a review of STM techniques see C. Julian Chen, *Introduction to Scanning Tunneling Microscopy*, Oxford Series in Optical and Imaging Sciences, Oxford Univ. Press, New York USA, (1993).

(8) H.W. Fink, W. Stocker and H. Schmid, Phys. Rev. Letters, **65**, 1204 (1990); J. Vac. Sci.Technol. **B8**, 1323 (1990); La Recherche, **22**, 964 (1991).

(9) J.C.H. Spence, W. Qian, J. Liu and W. Lo, Proc. 51st Annual Meeting of the Microscopy Society of America, 1060 (1993).

(10) For example see P.W. Hawkes and E. Kasper, *Principles of Electron Optics*, Vol. 1&2 , Academic Press 1989.

(11) Vu Thien Binh, N. Garcia, S.T. Purcell and V. Semet, *Nanosources and manipulation of atoms under high fields and temperatures: Applications*; pp. 56-76, Eds. Vu Thien Binh, N. Garcia and K. Dransfeld, Kluwer Series E: Applied Sciences - Vol. 235, Dordrecht, 1993.

(12) N. Garcia and H. Rohrer, J. Phys.: Condens. Matter **1**, 3737 (1989).

(13) R.D. Young, Rev. Sci. Instruments, **37**, 275 (1966)

(14) R.P. Feynman, R.B. Leighton and M. Sands, *The Feynman Lectures in Physics*, Addison Wesley Pub. Co. London, Vol. II (1964).

(15) The sample preparation is due to R. Semet and Pham Quang Tho of the Service Central d'Analyse Service d'Instrumentation (CNRS Solaize), France